A&A 470, 1023–1029 (2007)
DOI: 10.1051/0004-6361:20077365

Astronomy & Astrophysics

Optical variabilities in the Be/X-ray binary system

GRO J2058+42 (CXOU J205847.5+414637)

Ü. Kızıloğlu, N. Kızıloğlu, A. Baykal, S. K. Yerli, and M. Özbey

Physics Department, Middle East Technical University, Ankara 06531, Turkey
e-mail: umk@astroa.physics.metu.edu.tr

Received 27 February 2007 / Accepted 28 April 2007

ABSTRACT

Aims. We present an analysis of long-term optical monitoring observations and optical spectroscopic observations of the counterpart to CXOU J205847.5+414637 (high-mass X-ray binary system). We search for variability in the light curve of Be star.
Methods. We used differential magnitudes in the time-series analysis. The variability search in the optical light curve was made by using different algorithms. We used MIDAS and its suitable packages to reduce and analyse the spectra.
Results. We have performed a frequency search that gave us the value 2.404 d^{-1}. This value is attributed to the non-radial pulsation of the Be star. The Hα emission line profiles always show double-peaked emissions with a mean equivalent width of 2.31 ± 0.19 Å and a peak separation of 516 ± 45 km s^{-1}. This suggests that the Be star disk is still present. CXOU J205847.5+414637 is in an X-ray quiescent state.

Key words. stars: emission-line, Be – stars: early-type – stars: oscillations – X-rays: binaries

1. Introduction

The Be/X-ray binaries consist of a Be star and a neutron star that has little influence on the Be star. Be stars are on or just off the main sequence and they have rapid rotational velocities. The majority of them are found to rotate at 0.7 of their break-up velocity (Porter & Rivinius 2003). The Hα emission line and infrared excess are the observational characteristics of Be stars. Their emission lines disappear and reappear. Be stars often display enhancement or fading of their brightness. It is thought that enhancements in brightness are associated with the mass-loss episodes and appear to be induced by non radial pulsations (Rivinius et al. 2003). The spectroscopic variabilities in some line profiles are interpreted as due to non radial pulsations (Rivinius et al. 2003; Neiner et al. 2005). A Be star has a dense disk in its equatorial plane (Quirrenbach 1997; Waters 1986) that is fed from the material expelled from the fast-rotating Be star due to either radiatively driven wind or photospheric pulsations (Porter & Rivinius 2003). The favored disk model is the viscous disk model (Lee et al. 1991; Okazaki 2001). Quasi-Keplerian disks are held by viscosity (Okazaki & Negueruela 2001; Okazaki 2001) and the angular momentum is transferred from the inner regions of the disk towards the outer region by the viscosity. This disk causes the X-ray outburst of NS either at the periastron passage (type I outburst) or alters the outer part of the disk (type II outburst) without showing any correlation with orbital parameters (Negueruela 2004). X-rays are produced as a result of the accretion of matter onto the NS. In a Be/X-ray system, there can be X-ray quiescence periods, although a Be disk is present (Negueruela & Okazaki 2001; Negueruela et al. 2001).

The transient 198 s X-ray pulsar, GRO J2058+42 (CXOU J205847.5+414637), was discovered by the BATSE instrument on the Compton Gamma Ray Observatory during a giant outburst in September 1995 (Wilson et al. 1996). Wilson et al. (1998) propose that GRO J2058+42 was undergoing periastron and apastron outbursts on a 110-day orbit. They estimated its luminosity as 0.2–1 × 10^{37} erg/s, and no optical counterpart has been identified. Corbet et al. (1997) show the presence of modulation with a period of approximately 54 days in the analysis of RXTE/ASM (Rossi X-ray Timing Explorer/All Sky Monitor) data obtained between 1996 and 1997. Reig et al. (2004a) performed optical photometric and spectroscopic observations of the best fit to GRO position of the GRO J2058+42. They suggest that the star located at $\alpha = 20^{h}58^{m}47^{s}$, $\delta = +41°46'36''$, is the most likely optical counterpart. Spectra of the proposed star show a double-peak Hα emission profile with a mean equivalent width of 4.5 Å, which supports its classification as a Be/X-ray binary.

Subsequent Chandra observations did not find a source within the GRO positional error-box, but just outside, named CXOU J205847.5+414637. Wilson et al. (2005) obtained optical observations of CXOU J205847.5+414637. Its optical spectrum contained a strong Hα line in the double-peaked emission. They propose that CXOU J205847.5+414637 and GRO J2058+42 are the same object and classify the spectral type of this object as O9.5-B0IV-V ($V = 14.9$). They estimate the distance as 9 ± 1.3 kpc. When RXTE/ASM data for GRO J2058+42 were folded at a 55.03 d period, pulsation from this source was detectable in the 1996−2002 data, but was not present in 2003−2004 observations. This system has been in the X-ray quiescent phase since 2002. During the X-ray quiescence phase, the Be disk was present, since Hα was in emission as seen from their spectroscopic study (Wilson et al. 2005).

Short-term variabilities have been detected in several Be stars, especially in most early type Be stars. Baade (1982) attributed the short-term periodic line profile variabilities on timescales between 0.5 and 2 days to non-radial pulsations. Balona (1990) argued that periods were better explained by

stellar rotation, and he attributed LPV (line profile variability) to stellar spots. Guerrero et al. (2000) report the optical variability of the Be star o And during the period 1975−1998 and conclude that neither multimodal pulsations nor rotational modulation completely explain the complex light curves. Photometric variabilities in visual bands on timescales as short as one day are reported by Percy et al. (1997) for a sample of Be stars. Multiperiodicity has been detected in several Be stars in optical LPVs (Rivinius et al. 1998; Floquet et al. 2002; Neiner et al. 2005) and in photometric variabilities (Gutierrez-Soto et al. 2006) with periods few hours. Rivinius et al. (2003) report that the short-term periodic LPV of Be stars was due to non radial pulsation, which is thought to have a connection with mass loss or circumstellar disk formation. In addition to this they note secondary (transient) periods that were attributed to processes that strongly interact with or reside in the disk. They were formed in the photosphere and the close circumstellar environment. These periods were within 10% of the main photospheric period in their sample Be stars.

There is no long-term optical monitoring of this system, so in this study we present optical observations obtained by the ROTSEIIId telescope. The coordinates of CXOU J205847.5+414637 were taken from Reig et al. (2004a) and Wilson et al. (2005). We present optical spectroscopic observations obtained in 2006. We report the short-term variabilities seen in the optical light curve. From the analysis of archival RXTE/ASM observations, we attempt to detect the orbital modulation in 2005 and 2006.

2. Observations and data reduction

The optical data were obtained with Robotic Optical Transient Experiment[1] (ROTSEIIId) and Russian-Turkish 1.5 m Telescope[2] (RTT150) located at Bakırlıtepe, Antalya, Turkey.

2.1. Optical photometric observations

The CCD observations were obtained between Jan. 2005 and Aug. 2006 with 45 cm the ROTSEIIId robotic reflecting telescope. ROTSEIII telescopes that operate without filters are described in detail by Akerlof et al. (2003). ROTSEIIId is equipped with a 2048 × 2048 pixel CCD. The pixel scale is 3.3 arcsec per pixel for a total field of view $1\overset{\circ}{.}85 \times 1\overset{\circ}{.}85$. A total of about 1440 CCD frames were collected during the observations. In 2006, we had ∼400 data points. Due to the other scheduled observations and atmospheric conditions, we obtained 1−20 frames each night with an exposure time of 20 s. All images were automatically dark- and flat-field-corrected by a pipeline as soon as they were exposed. Dark field frames that were accumulated each night were used in the data reduction pipeline, together with proper sky-flat and fringe frames. For each corrected image, aperture photometry was applied using a 5 pixel (17 arcsec) diameter aperture to obtain the instrumental magnitudes. These magnitudes were calibrated by comparing all the field stars against the USNO A2.0 *R*-band catalog. Barycentric corrections were made to the times of each observation by using JPL DE200 ephemerides prior to the analysis with the period determination methods. Details on the reduction of data were described in Kızıloğlu et al. (2005) and Baykal et al. (2005).

[1] http://www.rotse.net

[2] http://www.tug.tubitak.gov.tr

Table 1. CXOU J205847.5+414637 and photometric reference stars.

Star	RA (J2000.0)	Dec (J2000.0)	USNO A2 *R* mag
J205847.5+414637	$20^h58^m47\overset{s}{.}54$	$+41°46'37\overset{''}{.}3$	14.4
Star 1	$20^h58^m53\overset{s}{.}53$	$+41°46'28\overset{''}{.}0$	13.9
Star 2	$20^h58^m45\overset{s}{.}85$	$+41°45'06\overset{''}{.}0$	13.9
Star 3	$20^h59^m05\overset{s}{.}50$	$+41°44'20\overset{''}{.}1$	14.1

We used differential magnitudes in the time series analysis. In magnitude measurements of ROTSEIIId, the magnitude determining accuracy decreases for fainter stars (Fig. 5 of Kızıloğlu et al. 2005). CXOU J205847.5+414637 has a moderate brightness, so use of fainter stars than our target as a reference may contribute significantly to the uncertainties of individual points in the differential light curve. When there are suitable stars available within the frame, it is better to choose reference stars that are brighter than the target so as not to introduce an additional noise into the light curve of the target. We adopted three stars as the reference, whose properties are given in Table 1, and we used their average light curve in order to reduce long-term systematic errors. We checked the stability of the reference stars and two test stars. The mean magnitude of reference stars (see Fig. 1) were used in the calculation of differential magnitudes.

2.2. Optical spectroscopic observations

The spectroscopic observations were performed with RTT150 on May 23, Jun. 16, Jul. 29, Aug. 19, and Sep. 26, 2006 using medium-resolution spectrometer TFOSC (TÜBİTAK Faint Object Spectrometer and Camera). The camera is equipped with a 2048 × 2048, 15 μ pixel Fairchild 447BI CCD. We used grisms G7 (spectral range 3850−6850 Å), G8 (5800−8300 Å), G14 (3275−6100 Å) and G15 (3300−9000 Å). The average dispersions are ∼1.5, ∼1.1, ∼1.4, and ∼3 Å pixel^{-1} for G7, G8, G14, and G15 respectively. We have a low signal-to-noise ratio for both May and June 2006 observations due to problems with the autoguider. The reduction and analysis of spectra were made using MIDAS[3] and its packages: Longslit context and ALICE.

3. Long-term monitoring

The differential optical light curve and X-ray light curve of Be/X-ray binary system CXOU J205847.5+414637 are shown in Fig. 1. The X-ray light curve was obtained from the RXTE/ASM web site[4]. The X-ray data covers the high-energy range (5−12 keV). Due to a varying amount of circumstellar matter, long or short-term variabilities are expected. These variabilities include both photospheric and circumstellar variabilities; therefore, a time series analysis of the observational data was performed.

3.1. Variability

We searched for variability in the light curve of Be star by using several different algorithms: Lomb-Scargle (Scargle 1982), Clean (Roberts et al. 1987), and Period04 (Lenz & Breger 2005)[5]. These methods were applied to all the observational data

[3] http://www.eso.org/projects/esomidas/

[4] http://xte.mit.edu

[5] Available at http://www.univie.ac.at

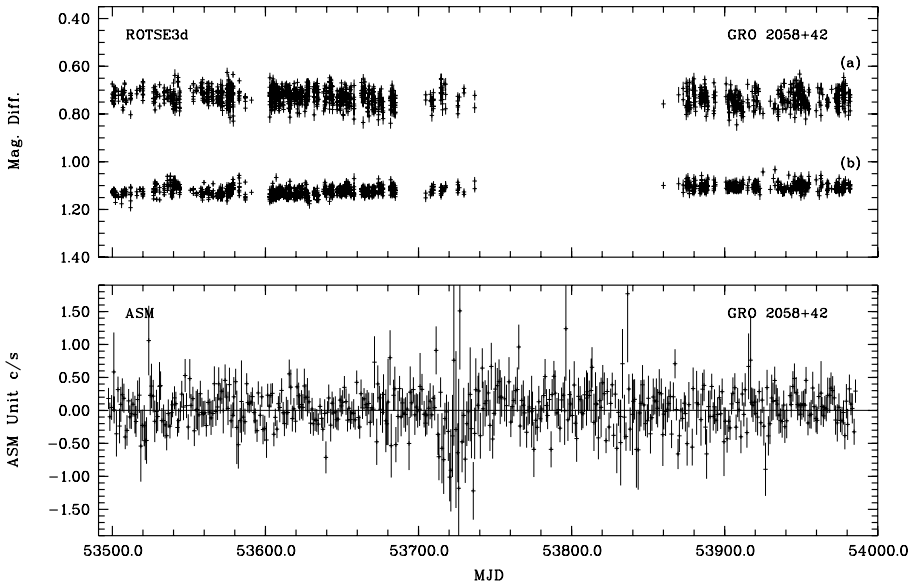

Fig. 1. ROTSEIIId differential light curve of the Be/X-ray binary system (*top panel* **a)**) and mean light curve of reference stars properly offsetted (*top panel* **b)**) for the period 2005−2006. The X-ray light curve of the system obtained from RXTE/ASM data is given in the bottom panel for the same time interval as ROTSEIIId observations.

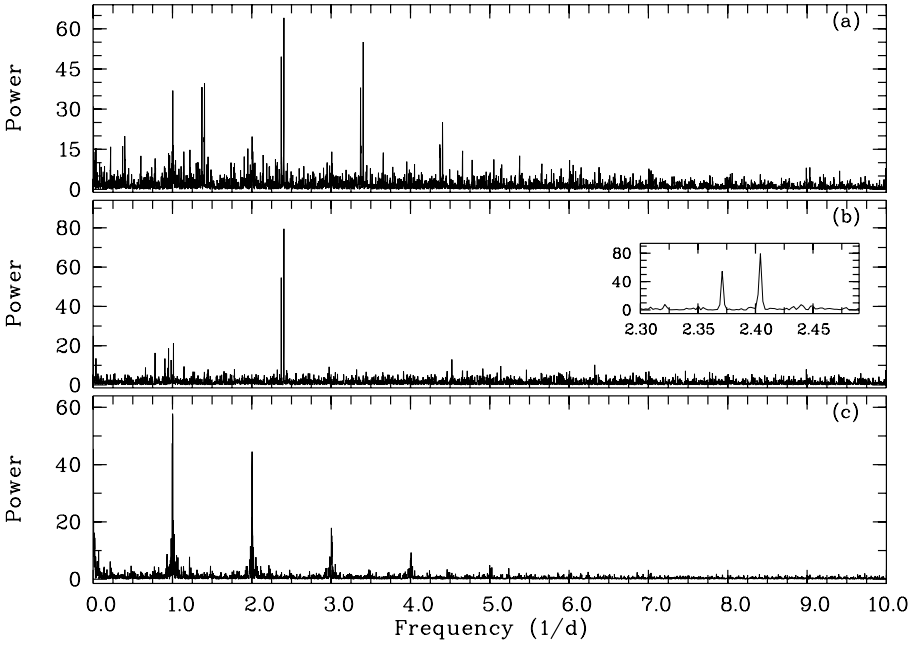

Fig. 2. Power spectra for the optical counterpart to CXOU J205847.5+414637. Panel **a)** Lomb-Scargle algorithm; **b)** Clean algorithm. Frequencies 2.404 and 2.371 d^{-1} are shown in the inset of the middle panel for clarity. The lower panel **c)** is the power spectrum of reference stars used in this study.

(from MJD 53499 to MJD 53982). Frequency analysis was performed over a range from 0 to 10 d^{-1} with a step width $1/T_{obs}$ = 1/476 = 0.0021 d^{-1}. Figure 2 shows the power spectra of the Be star (optical counterpart to CXOU J205847.5+414637). There is a very pronounced window function of one day, as expected due to a long observation period. Hence, aliases as a result of window function should be taken into account.

As seen from Fig. 2, the search for frequencies by performing Lomb-Scargle and Clean algorithms results with the same frequencies. The calculated frequencies are 2.404 and 2.371 d^{-1}. Periodogram analysis with Period04 confirmed these frequencies. The power spectrum of the mean light curve of reference stars obtained by LS algorithm is also shown in Fig. 2. Test stars gave similar results. Neither the reference stars nor the test stars show pronounced periodicities other than one-day aliases. There is no sign of frequencies 2.371 and 2.404 d^{-1}. However, the significance levels of the oscillations at 2.371 and 2.404 d^{-1}, which are present in both LS and cleaned spectra, should be set to provide convincing evidence of their reality. In Fig. 3a the log-log binned Lomb-Scargle periodogram of CXOU J205847.5+414637 is presented. As one can notice from the figure, a red noise component in the power spectra is seen between ∼1−8 d^{-1} with a power-law index $f^{-0.004}$. Even though the red noise component has a very low power-law index, we modeled the power spectrum in order to test the significance of these oscillations. In modeling the broad band continuum spectrum, we rebinned the power spectrum by a factor of 10. Then we modeled the broad band continuum by a Lorentzian centered at ∼0.6 d^{-1} with a *FWHM* ∼ 10.04 d^{-1}. As seen from the figure, we were able to model in this way both low-frequency (<1.0 d^{-1}) and red noise (between 1 and 8 d^{-1}) trends.

To test the significance of oscillations, the unbinned power spectrum is divided by its continuum model, and the resulting spectrum is multiplied by a factor of 2 (see van der Klis 1989; İnam et al. 2004, for applications). The resulting power spectrum (modified white noise model, MWN) would be a Poisson distribution for 2 degrees of freedom (d.o.f.). In this presentation, 5σ detection level of continuum normalized power is ∼44.

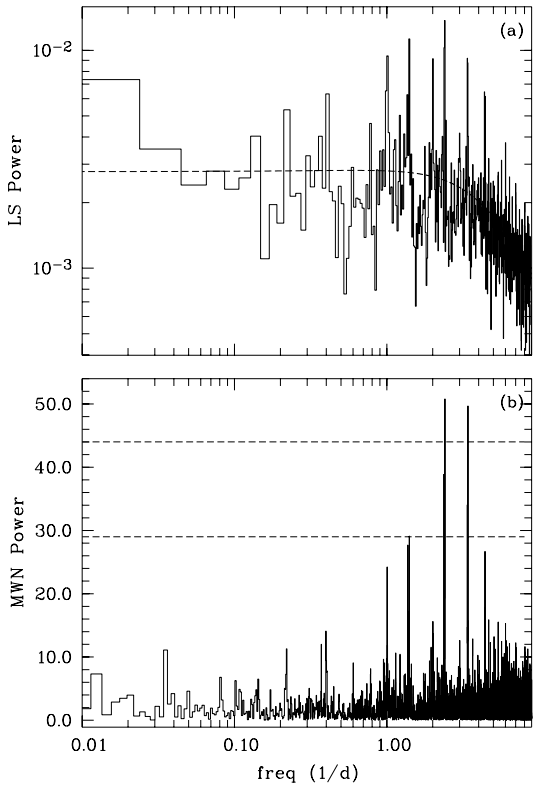

Fig. 3. *Upper panel*: the binned LS periodogram of counterpart to ROTSEIIId data of CXOU J205847.5+414637. A red noise component of a very low power index is seen in the 1–8 d^{-1} portion of the spectra. The dashed line represents the model continuum spectra as explained in the text. **b)** Below is the same power spectra normalized to the model continuum and multiplied by 2 to represent a Poisson distribution for 2 degrees of freedom. 3σ and 5σ confidence levels for the modified white noise model are denoted by dashed lines.

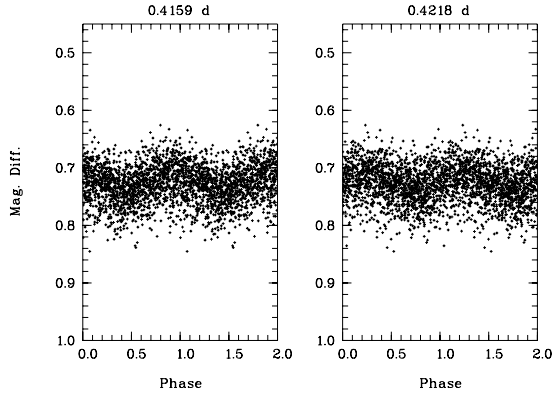

Fig. 4. The phase diagrams of 0.416 d and 0.422 d periodic variability for the differential light curve shown in Fig. 1.

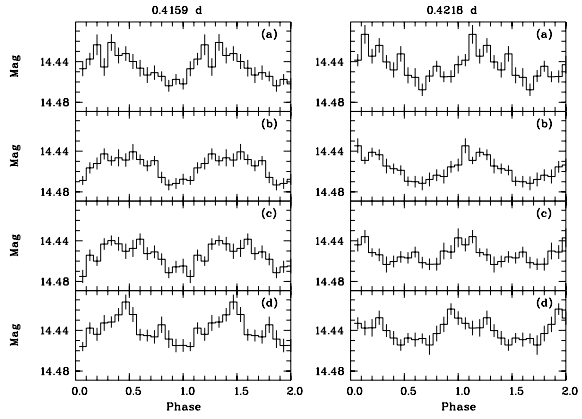

Fig. 5. The phase diagrams of 0.416 d and 0.422 d periodic variabilities for the time intervals as mentioned in the text, starting from MJD 53499 **a)** to MJD 53982 **d)**.

At this level the probability of detecting a false signal is $Q(44|2) \sim 2.7 \times 10^{-10}$. Since we have 4822 frequencies (the number of independent Fourier steps) in the power spectra, the probability of having a false signal becomes $4822 \times 2.7 \times 10^{-10} \sim 1.3 \times 10^{-6}$. This corresponds to the significance of signal detection of $1-1.3 \times 10^{-6} = 0.999999$. In Fig. 3b, we present the confidence levels of the observed oscillations. Only 2.404 d^{-1} has a confidence level greater than 5σ. The 2.371 d^{-1} frequency is in between the 3σ and 5σ confidence levels. Other frequencies are aliasing due to the observation window and are successfully removed, which can be seen in the cleaned spectra (Fig. 2b).

The phase diagrams of the 0.416 d (2.404 d^{-1}) and 0.422 d (2.371 d^{-1}) periods calculated from the time series shown in Fig. 1 are presented in Fig. 4. The mean amplitude of the oscillations are 13.4 ± 1.2 and 10.4 ± 1.2 mmag, respectively. To check the stability of the pulsations in 2005 and 2006, we used target time series so that only the uncertainties of target measurements will contribute to noise. In Fig. 5 we present the same phase diagrams calculated from the target time series. These phase diagrams are obtained by dividing the whole data into four parts (part a: MJD 53499-53583, part b: MJD 53586-53634, part c: MJD 53637-53736, part d: MJD 53836-53982). Each part has almost the same number of data points in order to get similar uncertainties in each bin. The periods are epoch-folded using the epoch T = MJD 53300. It is shown that the observed periods have coherent phase distributions during the different observation spans, in 2005 and 2006.

Short-term variabilities have already been found in most of the early type Be stars (Baade 1982; Rivinius et al. 1998; Floquet et al. 2002; Neiner et al. 2005). The timescales range from minutes to a few days and show either the photosphere or the circumstellar environment as their formation region (Porter & Rivinius 2003). Štefl et al. (2003) suggest that transient periods appear during or shortly after outbursts. In this study, our calculated frequency of 2.404 d^{-1} does not show a transient character so it can be attributed to the non-radial pulsation of Be star. If it were a transient frequency, then it should not re-appear with the same frequency and phase at a later epoch.

Periodic variabilities have not been detected in other Be/X-ray binary systems. It is believed that the companion has little influence on the Be star and alters only the outer part of the circumstellar disk. Then it is possible for Be stars in binary systems to exhibit periodic variabilities. There was a proposed periodic optical variability detection for the Be/X-ray binary system 2S 0114+65 by Taylor et al. (1995) with a period of 2.77 h and with a semiamplitude of 4 millimag. The evidence that this short-timescale variability in optical line profiles occurs was marginal in the study of Koenigsberger et al. (2003).

No long-term variabilities were found in the optical light curve. This shows that the disk was not changing very much over the time of observations.

Table 2. Journal of spectroscopic observations for the Hα line.

Date	MJD	Grism[a]	Exp. (s)	*FWHM* (Å)	*EW* (Å)	Δv (peak sep) (km s^{-1})
2006 May 23	53878	G7	4 × 600	15.8 ± 6.6	2.34 ± 0.27	–
2006 June 16	53902	G8	3 × 600	10.3 ± 4.3	2.42 ± 0.29	539.4
2006 July 29	53945	G7	2 × 1200	10.0 ± 4.1	2.31 ± 0.18	542.6
		G8	2 × 1800	11.0 ± 4.7	2.20 ± 0.17	516.9
		G15	1800	20.1 ± 8.4	2.65 ± 0.18	–
2006 August 19	53966	G8	1800	10.6 ± 4.4	2.03 ± 0.19	516.1
2006 September 26	54004	G8	1800	11.1 ± 4.7	2.58 ± 0.15	465.8
		G14[b]	3600	–	–	–

[a] Nominal dispersions for G7, G8, G14, and G15 are ∼1.5, 1.1, 1.4, and 3 Å pixel^{-1}, respectively. Hence, 3 pixel resolutions at the Hα line are: G7: ∼4.5 Å, G8: ∼3.4 Å, G14: ∼4.2 Å and G15: ∼9.1.
[b] G14 is sensitive in 3275–6100 Å band and used for blue spectra.

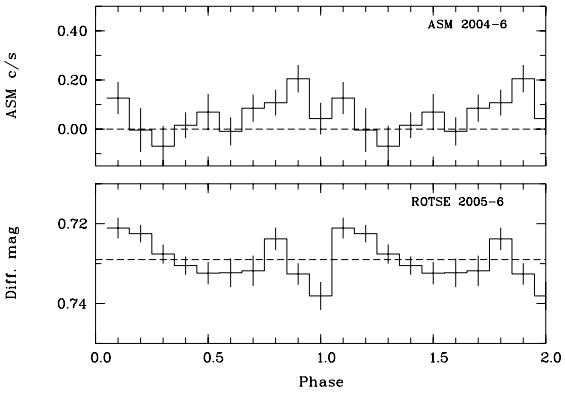

Fig. 6. Epoch-folded orbital phase of the Be/X-ray binary system CXOU J205847.5+414637 for RXTE/ASM and ROTSEIIId data (using the ephemeris T = MJD 50411.3 + 55.03N given by Wilson et al. 2005).

3.2. Orbital period signatures and X-ray quiescence

Before the year 2002 this system displayed type I outbursts in X-rays (Wilson et al. 2005) due to accretion of matter from Be disk at periastron passages. Between 2002–2004, type I outbursts were not seen and the orbital period was detected below 3σ level in the work of Wilson et al. (2005). We present 2004−2006 RXTE/ASM data (in the energy band 5–12 keV) folded at the orbital period of 55.03 d using the ephemeris given by Wilson et al. (2005) (T = MJD 50411.3 + 55.03N) in Fig. 6. In order to see whether there is any orbital period signature in optical light curve or not, we also folded the optical light curve at a period of 55.03 d using the same ephemeris and show the result in the bottom panel of Fig. 6. The RXTE/ASM data show no correlation with the ROTSE data. The power spectrum of the ASM data is just noise, all of which confirms that the cessation of activity, first noted by Wilson et al. (2005), has continued in subsequent years.

4. Analysis of spectra

The emission lines of the Be stars, particularly Hα (λ = 6563 Å), can be used for the existence of circumstellar disk of Be stars. We observed the counterpart of CXOU J205847.5+414637 to see whether any variability exists on the circumstellar disk. The journal of spectroscopic observations are listed in Table 2. The broadband (4500−7500 Å) low-resolution spectrum of the counterpart is shown in the upper panel of Fig. 7 for the July 2006 observation. Several features are recognized in addition to strong Hα line emission. In the lower panel of Fig. 7, Hα emission with a split profle is visible, together with the HeI λ6678 line (the resolution is ∼1.1 Å at Hα). The Hα profiles obtained from each spectrum are presented in Fig. 8. Table 2 gives the measurements of the equivalent width (*EW*) of the Hα line for each observing run and the values of full width at half maximum (*FWHM*) and the peak separation (Δv). The *FWHM* values are obtained from model calculations of the emission features. The mean *FWHM* calculated from G7 and G8 observations of June, July, August, and September 2006 is 10.6 ± 4.4 Å. May and June 2006 observations have a relatively low signal-to-noise ratio. The Hα line shows a double-peaked emission profile with a mean equivalent width of 2.31 ± 0.19 Å and peak separation of 516 ± 45 km s^{-1}. The mean equivalent width is almost half the values obtained by Wilson et al. (2005). The Hα line profiles in all runs show a self-absorption at the center of line due to the high inclination angle of the Be disk. The central absorption with a varying level in each observation reaches the continuum on July 2006. We could not detect whether night-to-night variations of Hα emission line exist, which would imply global structural changes of the disk.

The optical counterpart of CXOU J205847.5+414637 is in still a relative optic quiescence phase. However the depth of the self absorption feature in the middle of split Hα emission is deeper than the feature shown for July 2004 observation of CXOU J205847.5+414637 by Wilson et al. (2005). This can be interpreted as a decrease in the density of Be disk. Like Hα line, He I $\lambda\lambda$6678 and 7065 Å lines show emission peaks with central absorption.

The blue and mid-band spectra in Fig. 9 indicate several lines from the Balmer series (H9, H8, Hϵ, Hδ, Hγ, Hβ). The typical He I lines, $\lambda\lambda$4009, 4026, 4121, 4144, 4388 are shown in the lower panel. Weak or unresolved $\lambda\lambda$4437 and 4472 lines are also indicated. The other He I lines $\lambda\lambda$4713, 4922, 5016, and 5048 are shown in the upper panel of Fig. 9. Several DIBs are seen in blue, mid, and broad band spectra.

4.1. Rotational velocity

Be stars have rapid rotational velocities. They can be measured by using the empirical relation derived for the *FWHM* of He I lines (Steele et al. 1999). We calculated the rotational velocity $v \sin i$ = 241 ± 57 km s^{-1} by using He I lines $\lambda\lambda$4026, 4143, and 4471. This velocity is similar to the ones obtained in other Be systems (Nequeruela & Okazaki 2001; Reig et al. 2004b). We also calculated the rotational velocity from the

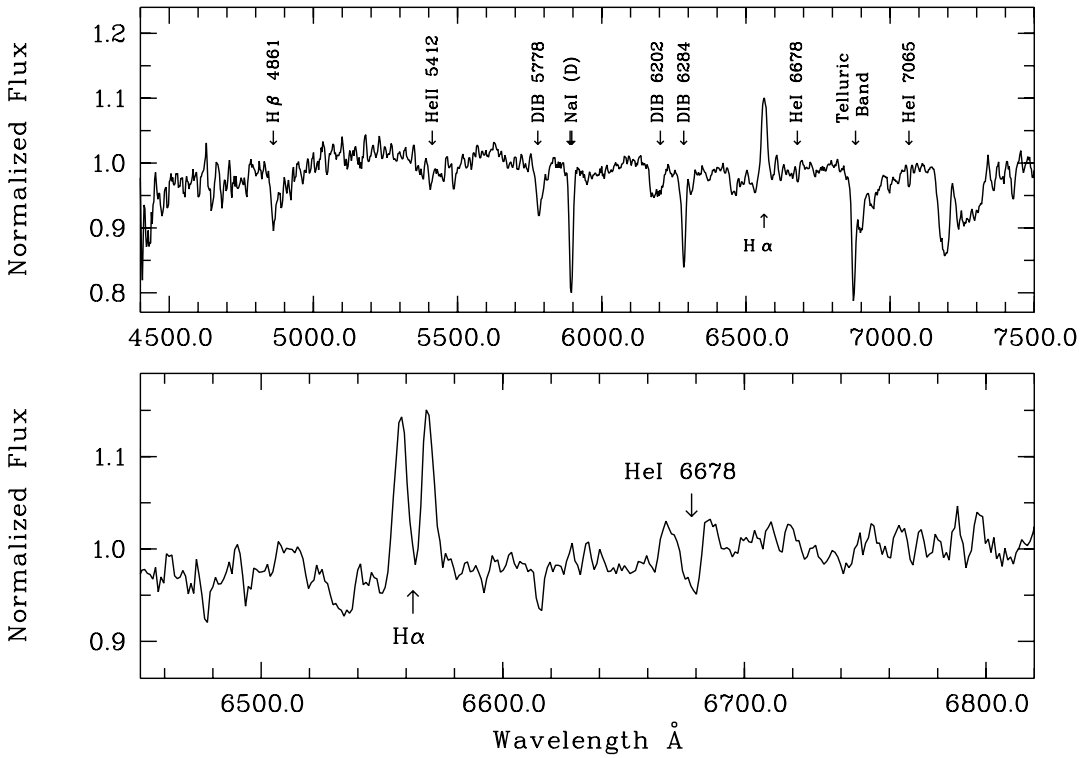

Fig. 7. Broadband (4500–7500 Å) (*top*) (with grism 15: resolution ~9.1 Å) and moderate resolution (*bottom*) (with grism 8, resolution ~3.4 Å) spectra of the counterpart to CXOU J205847.5+414637 taken in July 2006.

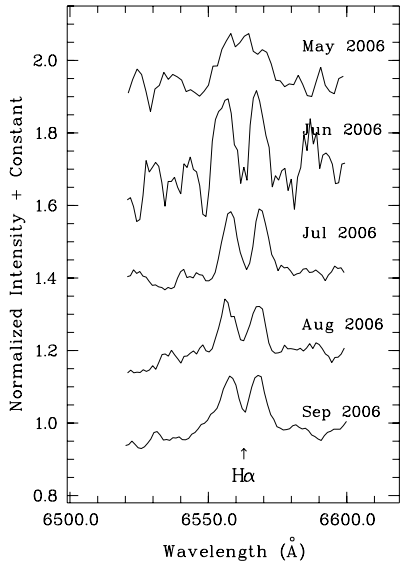

Fig. 8. Series of Hα profiles observed May–September 2006. Note low S/N for May and June data. The spectra correspond to the orbital phases of (*top to bottom*) 0.01, 0.45, 0.23, 0.61, and 0.30 which, are obtained using the ephemeris T = MJD 50411.3+55.03N given by Wilson et al. (2005).

average *FWHM* of Hα lines as $v \sin i$ = 242 ± 51 km s^{-1}. However the same velocity derived from the peak separation is found to be 258 km s^{-1}. On the other hand, using the equation given by Hanuschik (1989) (Eq. (1b): empirical relation between *FWHM* of Hα line and $v \sin i$ derived for a sample of 115 Be stars), we obtained the projected rotational velocity of the Hα emission region as $v \sin i$ = 312 km s^{-1}. All these calculations provide similar values. Calculation of the outer disk radius of the Hα emission region, derived from the peak separation values of Hα line (Coe et al. 2006), shows an increase in disk radius during our spectroscopic observation period.

5. Summary

By often displaying enhancement or fading of their brightness Be stars are candidates for a search for multi-periodicity. Multi-periodicity, which is mainly detected in optical LPV, has been generally attributed to non-radial pulsations. Pulsations combined with rapid rotation of Be stars are thought to be a prime candidate to explain mass loss and disk formation in Be stars. In this work, frequency analysis of the light curve of the Be star counterpart to CXOU J205847.5+414637 results in one short-term variability. The calculated frequency is 2.404 d^{-1}. This frequency is attributed to non-radial pulsation. The Be star has a $v \sin i$ value of about 250 km s^{-1} indicating an inclination angle greater than 40° (not to exceed the break-up velocity of Be stars) and can be easily placed in the defined band of Fig. 16 (photometric amplitude is plotted against $v \sin i$) of Rivinius et al. (2003).

The frequency 2.371 d^{-1}, which is very close to 2.404 d^{-1} as seen in Fig. 2, can also be thought of as a non-radial pulsation of this star. Its confidence is ~4σ. These frequencies do not show transient characteristics (Fig. 5). During different observation periods they appear with the same frequency and the same phase. Therefore the pulsations that we found are photospheric. The absence of outbursts supports the conclusion that the inner part of the disk is stable. The disk does not change very much over the time of observations.

We follow up the behavior of Hα line during the five months of 2006 by spectroscopic observations. Double-peaked Hα line profiles of a similar intensity remain unchanged during this period. We did not observe shell or single-peaked profiles. The self

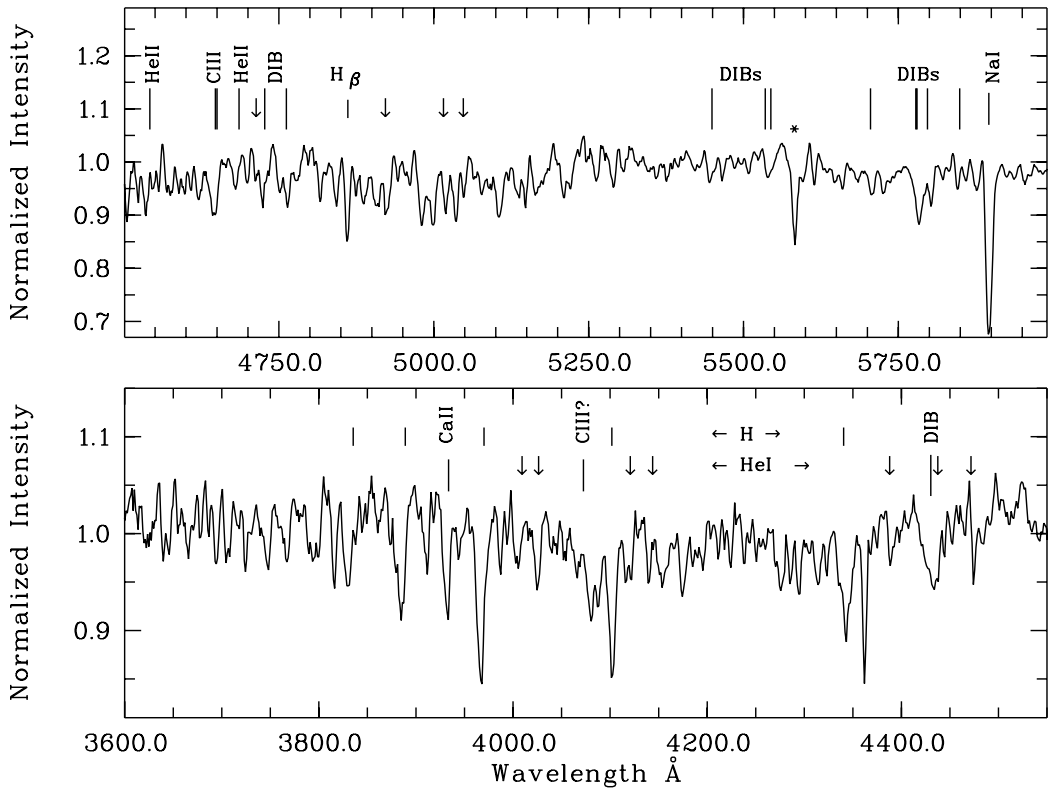

Fig. 9. Mid band (*top*) and blue (*bottom*) spectra for the optical counterpart to CXOU J205847.5+414637 taken on July 29 with grism 7 and on September 26 with grism 14. Both spectra have been normalized with a spline fit to continuum and smoothed with a median filter for display. Several strong lines from the Balmer series are indicated by short vertical bars. He I lines are shown by down arrows. Various other lines and DIBs are also indicated. "*" denotes the region affected by a cosmic ray hit.

absorption on the emission line, seen in our spectroscopic observations, is caused by the absorption of light coming from the interior part of the disk, by the outer regions of the disk. This occurs when the disk is under a large inclination angle *i*. The Be disk is still present. Our calculated *EW* values of Hα profiles are lower than the calculated values given by Wilson et al. (2005), indicating that Be star disk has lost some mass since 2004. It might also be possible that the density is lower, i.e. the disk grew and diluted or is a combination of less massive and less dense disk.

Acknowledgements. This project utilizes data obtained by the Robotic Optical Transient Search Experiment. ROTSE is a collaboration of Lawrence Livermore National Lab, Los Alamos National Lab, and the University of Michigan (`http://www.rotse.net`). We thank the Turkish National Observatory of TÜBİTAK for running the optical facilities. We thank the referee, Th. Rivinius, for a careful reading and valuable comments. Special thanks to Tuncay Özışık and colleagues from TUG who care for ROTSEIIId. We acknowledge support from TÜBİTAK, The Scientific and Technological Research Council of Turkey, through project 106T040. We also acknowledge the RXTE/ASM team for the X-ray monitoring data.

References

Akerlof, C. W., Kehoe, R. L., McKay, T. A., et al. 2003, PASP, 115, 132
Baade, D. 1982, A&A, 105, 65
Balona, L. A. 1990, MNRAS, 245, 92
Baykal, A., Kızıloğlu, Ü., & Kızıloğlu, N. 2005, IBVS, 5615
Coe, M. J., Reig, P., McBride, V. A., Galache, J. L., & Fabregat, J. 2006, MNRAS, 368, 447
Corbet, R., Peele, A., & Remilliard, R. 1997, IAUC, 6556
Floquet, M., Neiner, C., Janot-Pacheco, E., et al. 2002, A&A, 394, 137
Guerrero, G., Sareyan, J. P., Alvarez, P., et al. 2000, ASP Conf. Ser., 214, 205
Gutierrez-Soto, J., Fabregat, J., Suarez, J. C., et al. 2006, ASPC, 349, 249
Hanuschik, R. W. 1989, Ap&SS, 161, 61
İnam, C. S., Baykal, A., Swank, J., & Stark, M. J. 2004, ApJ, 616, 443
Kızıloğlu, Ü., Kızıloğlu, N., & Baykal, A. 2005, AJ, 130, 2076
Koenigsberger, G., Canalizo, G., Arrieta, A., Richer, M. G., & Georgiev, L. 2003, Rev. Mex. Ast. Astrof., 39, 17
Lee, U., Osaki, Y., & Saio, H. 1991, MNRAS, 250, 432
Lenz, P., & Breger, M. 2005, CoAst, 146, 53
Negueruela, I. 2004, in Proceedings of Massive Stars in Interacting Binaries, ed. N. St-Louis, & A. Moffat, ASP Conf. Ser., also in [arXiv:astro-ph/0411335]
Negueruela, I., & Okazaki, A. T. 2001, A&A, 369, 108
Negueruela, I., Okazaki, A. T., Fabregat, J., et al. 2001, A&A, 369, 117
Neiner, C., Floquet, M., Hubert, A. M., et al. 2005, A&A, 437, 257
Okazaki, A. T. 2001, PASJ, 53, 119
Okazaki, A. T., & Negueruela, I. 2001, A&A, 377, 161
Percy, J. R., Harlow, J., Hayhoe, K. A. W., et al. 1997, PASP, 109, 1215
Porter, J. M., & Rivinius, T. 2003, PASP, 115, 1153
Quirrenbach, A. 1997, ApJ, 479, 477
Reig, P., Kougenrakis, T., & Papamastorakis, G. 2004a, Atel, 308
Reig, P., Negueruela, I., Fabregat, J., et al. 2004b, A&A, 421, 673
Reig, P., Negueruela, I., Papamastorakis, G., Manousakis, A., & Kougentakis, T. 2005, A&A, 440, 637
Rivinius, Th., Baade, D., Štefl, S., et al. 1998, A&A, 333, 125
Rivinius, Th., Baade, D., & Štefl, S. 2003, A&A, 411, 229
Roberts, D. H., Lehar, J., & Dreher, J. W. 1987, AJ, 93, 968
Scargle, J. D. 1982, ApJ, 263, 835
Steele, I. A., Negueruela, I., & Clark, J. S. 1999, A&AS, 137, 147
Štefl, S., Baade, D., Rivinius, Th., et al. 2003, A&A, 411, 167
Taylor, M., Finley, J. P., Kurt, C., & Koenigsberger, G. 1995, AJ, 109, 396
van der Klis, M. 1989, in Timing Neutron Stars, ed. H. Ögelman, & E. P. J. van den Hauvel, NATO ASI Series (Kluwer), 27
Waters, L. B. F. M. 1986, A&A, 162, 121
Wilson, C. A., Strohmayer, T., & Chakrabarty, D. 1996, IAUC, 6514
Wilson, C. A., Finger, M. H., Harmon, B. A., Chakrabarty, D., & Strohmayer, T. 1998, ApJ, 499, 820
Wilson, C. A., Weisskopf, M. C., Finger, M. H., et al. 2005, ApJ, 622, 1024